DOI: 10.21917/ijivp.2020.0319

ENSEMBLE OF PREPROCESSING TECHNIQUES FOR 3D PALMPRINT RECOGNITION WITH COLLABORATIVE REPRESENTATION BASED CLASSIFICATION

Abdelouahab Attia[1], Abdelouahab Moussaoui[2], Youssef Chahir[3] and Mourad Chaa[4]
[1]*Computer Science Department, Mohamed El Bachir El Ibrahimi University of Bordj Bou Arreridj, Algeria*
[2]*Computer Science Department, Ferhat Abbas University, Algeria*
[3]*Department of Computer Science, University of Caen, France*
[4]*Faculty of New Technology of Information and Communication, Ouargla University, Algeria*

Abstract

3D Palmprint recognition has become a promising alternative tool for resolving problems compared to the robustness of 2D palmprint recognition. Regarding robustness, biometric systems that use 2D Palmprint suffer from being attacked by using a fake Palmprint identical. Given this, the current paper introduces a new 3D Palmprint recognition approach. Firstly, a set of preprocessing techniques has been applied on 3D depth image such as Tan and Triggs method which can effectively and efficiently eliminate the effect of the low-frequency component with keeping the local statistical properties of the processed image. Then, Gabor wavelets have been employed to extract features. After that, the extracted features have been used as an input in the collaborative representation based classification with regularized least squares (CRC_RLS) to classify the 3D Palmprint images. To evaluate its performance, the proposed algorithm has been applied on the PolyU 3D Palmprint database which contains 8.000 samples. The experimental results successfully and greatly improve the recognition results, especially when, we use Tan and Triggs method for preprocessing and Gabor for feature extraction with CRC_RLS for presentation and classification. We achieve a significant recognition rate of 100 % in lowest Runtime which reflects the robustness of the proposed recognition system.

Keywords:

Three-Dimensional Palmprint, Biometric, Gaussian Difference Filtering, Gradient Palms, Weberpalms, Gabor Features, Self-Quotient Image Algorithm

1. INTRODUCTION

Biometrics is a potentially powerful technology to respond to the security-related requirements. Effectively, different biometrics has been designed to use behavioral characteristics and/or physiological specific to each person. The major advantage of such features is being universal, unique, and permanent, instead of the classic means such as passwords or badges [1]. Therefore, several biometric techniques based on a set of biometric modalities such as palmprint, fingerprint, face, hand, iris, voice, signature and finger knuckle patterns (FKP) [2]-[6] have been widely applied in various applications in industries. With the emergence of 3D technology acquisition devices, the 3D palmprint shape has been introduced in the recognition problems and has been considered as a very promising way. A 3D Palmprint biometric system uses 3D imaging device to acquire depth information of human palm and uses this data in performing user identification. The main advantage of 3D model-based approaches is that the 3D model retains all the information on the palmprint geometry, which provides a real representation of the latter. However, the challenge is still open to this day, including (i) optimizing the computing time required in recognition scenarios and (ii) making 3D palmprint recognition systems more accurate and robust. To encounter these challenges, several methods have been developed.

Zhang et al. [7] have been extracted, for the first time, the Mean Curvature Image (MCI), Gaussian Curvature Image (GCI) and Surface Type (ST) features. These features have been used for the 3D palmprint recognition system. Given this, the Matching Score Fusion of MCI, GCI, and ST features have been discussed in this paper where Matcher Weighting (MW) provides the best result.

Zhang et al. [8] have developed a system for palmprint verification by using 2D and 3D features. The surface curvature features have been used as 3D representations. For the matching process, the normalized local correlation (LC) has been applied and the value of the matching score that used in the decision module.

Cui [9] have exploited both 2D and 3D features of palmprint to build an efficient multimodal recognition system in the matching score level. Then, both 2D and 3D features obtained by Principal Component Analysis (PCA) have been followed by two-phase test sample representation (TPTSR).

Meraoumia et al. [10] have combined both the 2D and 3D information of palmprint in order to build an efficient multimodal biometric system based on fusion at the matching score level. PCA and Discrete Wavelet Transform (DWT) have been used for feature extraction on palmprint images (2D or 3D) with a Hidden Markov Model (HMM) for modeling the feature vectors.

Zhang et al. [11] have introduced 3D palmprint identification system. Typically, the block-wise features have been employed for feature extraction and the collaborative representation (CR) based framework with $l1$-norm or $l2$-norm regularizations have been used for the classification stage.

Chaa et al. [12] introduced a novel method based on the score level fusion of 2D and 3-D palmprint for personal recognition systems. However, the self-quotient image (SQI) algorithm has been applied for reconstructing illumination-invariant 3-D palmprint images. Then, Gabor wavelets have been used to extract discriminative Gabor features from SQI images. Followed by the dimensionality reduction methods, a Principal Component Analysis (PCA) and Linear Discriminant Analysis (LDA) technique have been employed. In the matching stage, the cosine Mahalanobis distance has been applied.

The current paper proposes a simple and fast 3D Palmprint identification system. For 3D palmprint, several preprocessing techniques have been applied in face recognition but there are not

applied in 3D palmprint recognition. Thus, these algorithms have been used in 3D palmprint to extract the reflectance image. Consequently, the Tan and Triggs method (TT) has been used, because the illumination can be considered as the low-frequency component of the image. For that reason, we have excluded it. Then, several features extraction methods are defined and used to extract features from the processing images. Such as: Gabor wavelets, Histograms of Oriented Gradients (HOG), and Three-Patch Local Binary Pattern (TPLBP). The interest in choosing the TPLBP and Gabor based methods are both methods are invariant to monotonic illumination changes. Mainly, the proposed system consists of four main steps as illustrated in Fig.1.

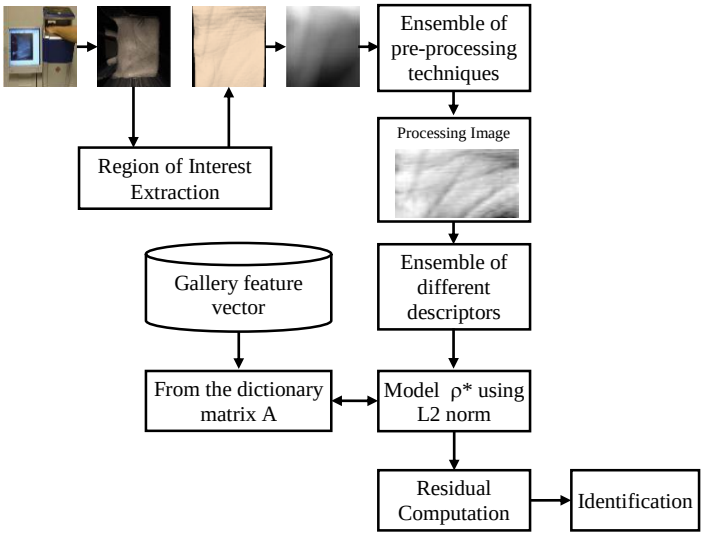

Fig.1. Block Diagram of the proposed method

First, the 3D palmprint images have been captured using a 3D palmprint acquisition device based on structured-light technology. This device was invented by Li et al [13]. Then, 3D region Of Interest (ROI) has been extracted. Next, an ensemble of preprocessing techniques has been applied on 3D ROI palmprint images for eliminating efficiently the effect of the low-frequency component with ensuring to keep the local statistical properties of the processed images. These techniques include Gaussian Difference Filtering [14], Tan and Triggs method [15], Gradient palms [16], the single scale weberpalms normalization technique [17] and the self-quotient image technique [18]. Then, different local descriptors; Gabor wavelets [19], Three-Patch Local Binary Patterns (TPLBP), The Histograms of Oriented Gradients (HOG) [21] have been used to extract features. Finally, the extracted features have been used by the Collaborative Representation based Classification with Regularized Least Squares (CRC_RLS) to classify the 3D palmprint images.

The rest of this paper is organized as follows: 3D palmprint recognition system is described in section 2. Mainly, it presents the different preprocessing techniques and the different feature extraction methods. Section 3 is devoted to the conducted experiments and the obtained results during the course of the experiments. Finally, section 4 provides an overall conclusion and directions improvement in the future.

2. PROPOSED METHOD

2.1 REGION OF INTEREST EXTRACTION

This section depicts the region of interest (ROI) extraction method for 3D palmprint. The 2D and 3D palmprint images are obtained all together, with a one-to-one matching between the 3D cloud points and the 2D pixels. Thus, the ROI of the 3D palmprint data can be easily extracted via the 2D palmprint ROI extraction process.

There are five major steps for ROI extraction, such as [7] [22]:

Step 1: Started by applying a Gaussian Smoothing Operation to the input image. Followed by, binarization of the smoothed image with a threshold H (Fig.2(a)-Fig.2(b)).

Step 2: Next, the boundaries of the binary image that simply extracted via a boundary tracking algorithm, as presented in Fig.2(c). After obtaining the boundaries of the gaps, (P_1, P_2) are noticed by (F_ix_j, F_iy_j) with (i =1,2), respectively.

Step 3: Calculate the tangent of the two gaps. Let (x_1,y_1) and (x_2, y_2) be any points on (F_1x_j,F_1y_j) and (F_2x_j,F_2y_j) respectively. If the line (y=mx+c) passing though these two points satisfies the inequality, $F_iy_j \leq mF_ix_j+c$, for all i and j (Fig.2(d)), then the line (y=mx+c) is considered to be the tangent of the two gaps.

Step 4: Line up (x_1,y_1) and (x_2,y_2) to get the Y-axis of the palmprint coordinate system, and use a line passing through the midpoint of these two points, which are perpendicular to the Y-axis, to determine the origin of the coordinate system. The ROI has been located by the rectangle (Fig.2(d)).

Step 5: Extract a sub-image of a fixed size based on the coordinate system. The sub-image is located at a certain area of the palmprint image for feature extraction Fig.2(e).

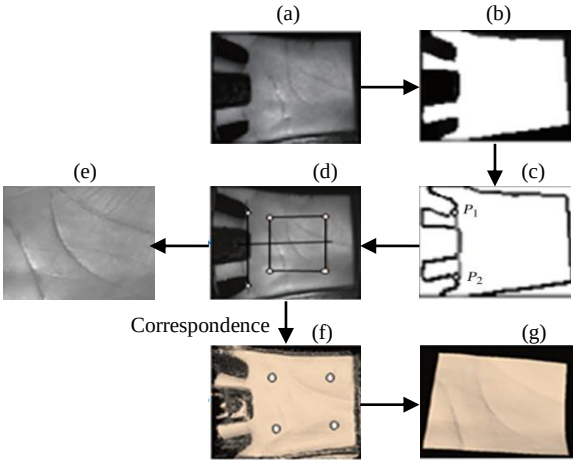

Fig.2. Steps of extraction ROI of 3-D palmprint image

The Fig.2(g) depicts the obtained 3D ROI by grouping the cloud points corresponding to the pixels in 2D ROI.

2.2 PREPROCESSING TECHNIQUES

2.2.1 Gaussian Difference Filtering (DoG):

In the processed step, the Gaussian Difference (DoG) filtering has been employed on image denoted as $I(i,j)$ using the following formula:

$$I_p(i,j)=DoG*I(i,j) \quad (1)$$

where *DoG* filter can be computed by using the following equation:

$$DoG=\frac{1}{2\pi\sigma_L^2}e^{-\frac{i^2+j^2}{2\sigma_L^2}}-\frac{1}{2\pi\sigma_H^2}e^{-\frac{i^2+j^2}{2\sigma_H^2}} \quad (2)$$

The DoG filter has been used as a band pass filter. Thus, σ_L and σ_H denote the low and high frequencies respectively. The cutoff frequencies should depend on the quality of the images. Information is mainly placed in bass frequency. Given this, choosing the value σ_L too much high will cause deletion of useful information. By varying these values in these intervals, slightly better results have been obtained at σ_H=10 and σ_L=0.1

2.2.2 Tan and Triggs Method (TT):

It has been done in three steps [15] [10]:

- *Gamma correction*: The first step is described by the mathematical relation:

$$I'(i,j)=I(i,j)^{\tau} \text{ where } \tau\in[0,1] \quad (3)$$

In the Eq.(3), $I(i,j)$ is the input image, $I'(i,j)$ denotes the image resulting from the first step of preprocessing and τ stands for the gamma value.

- *Difference of Gaussians*: consists of an implementation of a band pass to remove low frequencies containing the undesirable effects of shadows and high frequencies containing aliasing and noise.

Contrast equalization: is carried out in three stage as follows:

$$I(i,j)\leftarrow\frac{I(i,j)}{\left(mean\left(\left|I(i',j')\right|^{\alpha}\right)\right)^{\frac{1}{\alpha}}} \quad (4)$$

$$I(i,j)\leftarrow\frac{I(i,j)}{\left(mean\left(\min\left(\rho,\left|I(i',j')\right|^{\alpha}\right)\right)\right)^{\frac{1}{\alpha}}} \quad (5)$$

$$I(i,j)\leftarrow\rho\tanh\left(\frac{I(i,j)}{\rho}\right) \quad (6)$$

where α stands for the powerfully compressive exponent which decreases the influence of huge values. ρ refers to the threshold that is used to truncate the big values once the first stage of normalization, and then by default, we utilize α=0.1 and ρ=10.

2.2.3 Gradient Palms (GPs):

The GPs method was introduced by Zhang et al. [16]. Typically, the GPs has been used to get the Gradient palm image. However, the palm image has been smoothed by employing Gaussian Kernel function that is given in the Eq.(7):

$$I'(i,j)=I(i,j)*G(i,j,\sigma) \quad (7)$$

where $G(i,j,\sigma)$ represents the Gaussian Kernel function that is calculated by:

$$G(i,j,\sigma)=\frac{1}{2\pi\sigma^2}\exp\left(-\frac{i^2+j^2}{2\sigma^2}\right) \quad (8)$$

In the above equation, σ stands for the standard deviation of the Gaussian derivative filters that have been used for estimating the image gradient. Then, the orientation of the image gradients GP has been accomplished by using the following equation:

$$GP=\arctan\left(\frac{I'_y(i,j)}{I'_x(i,j)}\right) \text{ with } GP\in[0,2\pi] \quad (9)$$

where $I_x'(i,j)$ and $I_y'(i,j)$ are the gradient mages of $I'(i,j)$ in the x,y direction, respectively.

$$I'_x(i,j)=I'(i,j)*G_x(i,j,\sigma) \quad (10)$$

$$I'_y(i,j)=I'(i,j)*G_y(i,j,\sigma) \quad (11)$$

The single scale Weber palms normalization technique (WEBP)

The WEBP method was introduced by October et al. [19]. However, the WEBP has been used to obtain Weber palm image (WEBP). First, the depth 3D palmprint image has been smoothed by using a Gaussian filter as shown in the following equation:

$$F=F*G(i,j,\sigma) \quad (12)$$

where $G(i,j,\sigma)$ denotes the Gaussian Kernel function which is calculated by:

$$G_y(i,j,\sigma)=\frac{1}{2\pi\sigma^2}\exp\left(-\frac{i^2+j^2}{2\sigma^2}\right) \quad (13)$$

Then, the obtained F' image has been processed with weber local descriptor (WLD):

$$WEBP=WLD\left(F'(i,j)\right)=\arctan\left(\alpha\sum_{i\in A}\sum_{j\in A}\frac{F'(i,j)-F'(i-x\Delta i,j-y\Delta j)}{F'(i,j)}\right) \quad (14)$$

where A={-1,0,1} and α is a parameter for adjusting the intensity difference between neighboring pixels.

2.2.4 Self-Quotient Image:

In [18], the SQI algorithm was introduced to the field of face recognition by Wang et al. [18]. In this paper, the SQI algorithm has been used to extract the self-quotient image from each the Region of Interest (ROI) of 3D palmprint image. In general, a ROI palmprint image $I(i,j)$ at each point (i,j) is given by:

$$I(i,j)=R(i,j)\cdot L(i,j) \quad (15)$$

where $R(i,j)$ represents the reflectance image and $L(i,j)$ denotes the illuminance image. From Eq.(15), the reflectance image $R(i,j)$ is given by:

$$R(i,j)=I(i,j)/L(i,j) \quad (16)$$

Because illumination can be considered as the low-frequency component of the image $I(x,y)$, it can be then estimated as:

$$L(i,j)\approx F(i,j)*I(i,j) \quad (17)$$

where, $F(i,j)$ is a Gaussian filter with size sand standard deviation σ. * refers to the convolution operation.

From the Eq.(16) and Eq.(17), the self-quotient image $Q(i,j)$ is calculated as:

$$R(i,j) \approx Q(i,j) = \frac{I(i,j)}{F(i,j) * I(i,j)} \quad (18)$$

In the experiments stage, 3D ROI images and 2D ROI image shave been processed using a set of preprocessing techniques. In Fig.3, the 3D ROI palmprint images and their preprocessing images are clearly depicted.

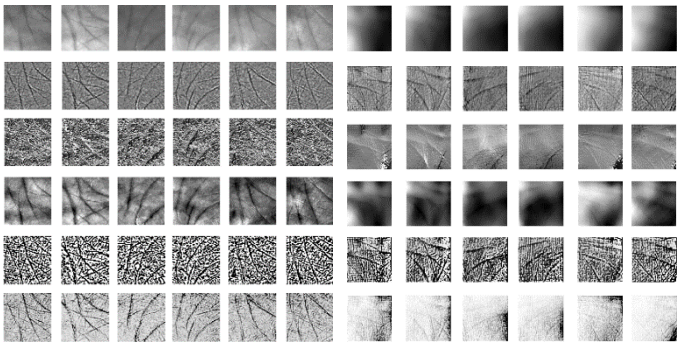

(a) (b)

Fig.3 (a) 2D palmprint images and (b) 3D palmprint images: 1st row: (a) samples of 2D ROI palmprint images. (b) Example of 3D depth ROI images.2nd row: their processing images using the TT method. 3rd row: their processing images using GPs method. 4th row: their processing images using DOG method. 5th row their processing images using WEBP method. 6th their processing images using SQI method

2.3 FEATURES EXTRACTION

Gabor wavelets have been used to extract features. According to October et al. [19] Gabor wavelets are well-known as away space-frequency analysis. Indeed, Gabor wavelets are a very robust method. This specificity has made Gabor filters as a powerful means of texture analysis and classification. Gabor filters analyze the texture of an image with the different resolutions and orientations. In the spatial domain, Gabor filters can be done by using the following Eq.(19):

$$H_{\mu,v} = \frac{f_\mu^2}{\pi n \lambda} \exp\left[-\left(\frac{f_\mu^2}{n^2} \right) x_p^2 - \left(\frac{f_\mu^2}{\lambda^2} \right) y_p^2 \right] \exp\left(j 2\pi x_p \right) \quad (19)$$

where

$x_p = x\cos(\theta_v)+y\sin(\theta_v)$ and

$y_p = -x\sin(\theta_v)+y\cos(\theta_v)$,

$f_\mu = f_{max}/2^{0.5\mu}$ and $\theta_v = \upsilon\pi/8$.

f_μ and f_{max} are the center and the maximal frequency, respectively and

θ_v stands for its orientation.

In the experiments, the parameters of 2D Gabor filters have been empirically selected such as the maximal frequency f_{max}=0.25 and $n=\lambda=\sqrt{2}$. n and λ refer to the size of the Gaussian envelope along x-axis and y-axis respectively.

The Gabor representation of preprocessing 3D image has been obtained by the convolution of the image with the family of Gabor filters (5 scales and 8 orientations). The 40 magnitude responses have been down-sampled with a factor 64 and normalized to zero mean and unit variance. Then, these responses have been transformed into a vector by scan columns. All vectors have been concatenated to produce the new feature for each palm. To give a comparison, another two algorithms have been used to extract the features: (i) The Histograms of Oriented Gradients (HOG) proposed by Dalal et al. [21] and (ii) Three-Patch Local Binary Pattern (TPLBP) proposed by Wolf et al. [20] .The parameters of TPLBP algorithm have been empirically selected as S=8, R=7, W=5, Alpha=1 and Grid=15. For HOG algorithm, they have been selected as 12 orientation bins, the size of HOG cell= [8 8] and the number of cells in block = [2 2].

2.4 COLLABORATIVE REPRESENTATION BASED CLASSIFICATION (CRC)

Assuming that $X=\{x_1,\ldots,x_n\} \in R^{d\times n}$ is given where x_i corresponds to d-dimensional training data, every x_i belongs to one of C classes where C denotes the number of classes varied from 1 to C. the notation n stands for the number of data.

Let $X_i \in R^{d\times n_i}$ be a set of training data from class i=1,2,…,C as soon as a test data $y \in R^d$ comes, we get y as follows $y=X\rho$, where ρ represents a set of parameters. Taking into account the minimum reconstruction error, the adequate values of ρ are given by resolving this equation:

$$\rho^* = \arg\min_\rho \|y - X\rho\|_2^2 \quad (20)$$

Here, the training data have been linearly combined to minimize the least square reconstruction error of the test data. It is worth noticing that the use of all training data to collaboratively represent test data lessens the small sample size problem in face recognition [22], CRC_RLS is given in [22] as follows:

$$\rho^* = \arg\min_\rho \left\{ \|y - X\rho\|_2^2 + \lambda \|\rho\|_2^2 \right\} \quad (21)$$

where λ stands for the regulation parameter. The Eq.(21) can be resolved analytically as follows:

$$\rho = \left(X^T X + \lambda \cdot I \right)^{-1} X^T y = Py \quad (22)$$

where P is a linear transformation matrix which is pre-calculated without considered y.

$$P = \left(X^T X + \lambda \cdot I \right)^{-1} X^T \in \mathbb{R}^{n\times d} \quad (23)$$

Hence, the class label of y in CRC_RLS method, is given by:

$$class(y) = \arg\min_i \left\{ \frac{\|y - X_i\rho_i\|_2}{\|\rho_i\|_2} \right\} \quad (24)$$

In the Eq.(24), ρ_i denotes a set of representation coefficients whose length is n_i. As mentioned in the geometrical analysis in [21], the least square term in Eq.(24) is effective and robust because the class label of y is identified from the minimum error among the class of wise reconstruction errors. It has been indicated that the division of the reconstruction error by $\|\rho_i\|_2$ yields additional discrimination information. For further information, the reader is invited to see the original paper [20].

3. EXPERIMENTAL RESULTS

The experiments have been carried out on the 3D or 2D ROI palmprint database collected by Hong Kong Polytechnic University (PolyU) (https://www4.comp.polyu. edu.hk/~biometri

cs) which contains 400 classes. In this work, 8, 0000 images have been used where each class is represented by 20 images. The palmprint images given in the first sessions have been taken as the gallery set in all the conducted experiments. The samples collected at the second session have been used as the probe set. As for the identification experiment, results have been presented recognition rate (*RR*) metrics. The *RR* is given by:

$$RR = \frac{N_i}{N} \cdot 100(\%) \tag{25}$$

where, N_i stands for the number of images effectively allocated to the right identity. *N* refers to the global number of images trying to assign an identity. The software MATLAB R2017a and Windows 7 operating system have been used to realize the introduced method. Experiments have been accomplished on a laptop Core i3-2375M CPU with 4Go MB RAM. Suppose a test data, the runtime for one identification operation including the time required by the feature extraction step and the time necessary for the matching step.

3.1 3D PALMPRINT EXPERIMENTS

The current section provides a comparison of different preprocessing techniques. The obtained results are depicted in Table.1. From, Table.1, it is clear that TT + Gabor + CRC_RLS method outperforms significantly the other four methods: MSWP + Gabor + CRC_RLS, DOG + Gabor + CRC_RLS, GPs + Gabor + CRC_RLS, and MSWEBP + Gabor + CRC_RLS.

In identification mode, the cumulative match characteristic (CMC) curves have been used, which represents performance curves for 3D palmprint biometric recognition systems. The ROR carries information about the percentage of traits, where the closest match in the stored database corresponds to the right identity, which is among the top r ranked matches with $r = 1, 2,...,$ *N* and *N* stand for the number of persons in the database.

Table.1 Recognition rate and runtime for different techniques.

Methods	RR (%)	Runtime for 1 identification (ms)
MSWP+Gabor+ CRC_RLS	99.85%	790
DOG+Gabor+CRC_RLS	99.20%	770
TT+Gabor+CRC_RLS	**100.00%**	330
GPs+Gabor+CRC_RLS	97.25%	1010
SQI+Gabor+CRC_RLS	97.85%	1460

Thus, Fig.4 shows the CMC curves of the 3D palmprint recognition system using different techniques. The Fig.4(a) depicts CMC plots of the ranking ability of a 1 to 100 identification system. It can be observed from Fig.4(a) that the best rank-1 recognition rate of the accuracy at rank 1, rank 10 and rank 100, is for the TT + Gabor + CRC_RLS compared to Gabor + CRC_RLS and CRC_RLS methods. This demonstrates the efficiency of the preprocessing technique TT method in improving the system accuracy. Thus, the performance gain by our method is over 6.60%. The Fig.4(b) presents the comparative performance using the preprocessing TT method with different descriptors. Thus, from these CMC plots of TT + Gabor + CRC_RLS, TT + TPLBP + CRC_RLS and TT + HOG + CRC_RLS. We can observe that we obtain significant gain at all ranks (1, 10 and 100) of TT + Gabor + CRC_RLS compared to TT + TPLBP + CRC_RLS and TT + HOG + CRC_RLS.

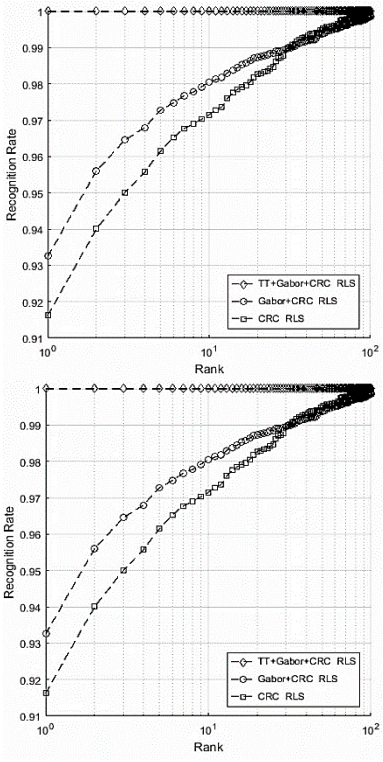

Fig.4. CMC curves for 3D palmprint using different techniques - A comparative performance

The coding coefficients $l1$ regularized of a query sample are shown in Fig.5(a) and Fig.5(b) shows the recognition rate versus the different values of λ using $l1$ normalization. The coding coefficients l2 regularized of a query sample are shown in Fig.6(a) and Fig.6(b) shows the recognition rate versus the different values of λ using $l2$ normalization.

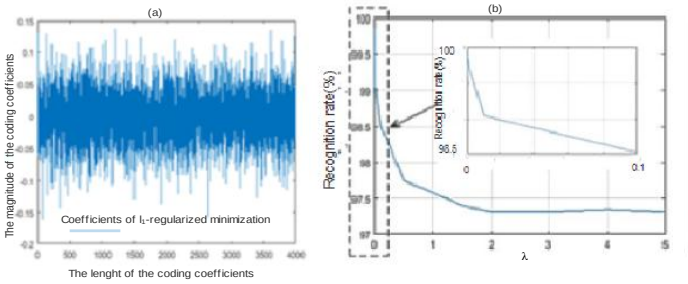

Fig.5(a). The coding coefficients $l1$ regularized of a query sample (b) Recognition rate versus the different values of λ using $l1$-normalization

The Fig.5(a) presents the coding coefficients $l1$ regularized of a query sample. Thus, we test the performance of ($l1$-regularized minimization) and (l2-regularized minimization) CRC-RLS with different values of regularization parameter λ in Eq.(21). The results on the PolyU 3D palmprint databases are shown in Fig.5(b) and Fig.6(b), respectively. From these plots, we observe that when λ=0, CRC-RLS will fail. When λ is assigned a small positive value, in the range of [0.00001 - 0.1], can be reached a high recognition rate. When λ is greater than 0.1 the recognition rate fall down. From Fig.5 (b) and Fig.6(b) we can find that with the

increase of λ(>0.1), no much benefit of recognition rate can be gained. In addition, the l2-regularized minimization CRC-RLS could get similar recognition rates to the l1-regularized minimization in a broad range of λ.

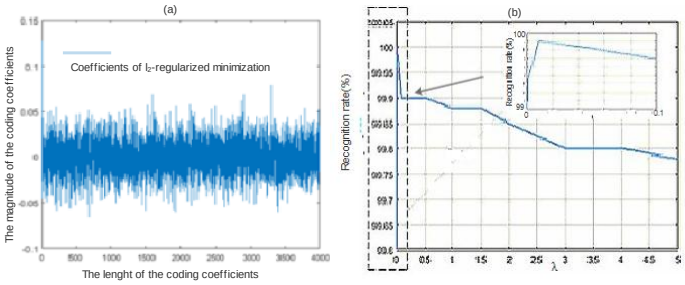

Fig.6(a). The coding coefficients l2 regularized of a query sample (b) Recognition rate versus the different values of λ using l2-normalization

A comparison in terms of recognition identification of the different preprocessing techniques has been performed. From Table.2, it is clearly noticed that TT + Gabor + CRC_RLS method performs significantly better than the other four methods:

- MSWP + Gabor + CRC_RLS
- DOG + Gabor + CRC_RLS
- GPs + Gabor + CRC_RLS and
- MSWEBP + Gabor + CRC_RLS.

The comparative results obtained before and after using TT processing are depicted in Table.3 where it is obviously seen that the use of the TT processing method improves the accuracy rate.

Table.2. Recognition rate with runtime for different techniques

Methods	RR (%)	Runtime for 1 identification (ms)
MSWP+Gabor+ CRC_RLS	100%	460
DOG+Gabor+CRC_RLS	99.98	560
TT+Gabor+CRC_RLS	**100%**	**560**
GPs+Gabor+CRC_RLS	99.92	700
MSWEBP+Gabor+CRC_RLS	100%	640

Table.3. Comparative results before and after preprocessing for 3D palmprint using different techniques

Before Pre-processing	RR (%)	Runtime for 1 Identif-ication (ms)	After Pre-processing	RR (%)	Runtime for 1 Identif-ication (ms)
Gabor+ CRC_RLS	99.95	430	TT+Gabor+ CRC_RLS	100	560
TPLBP+ CRC_RLS	99.80	2003	TT+TPLBP + CRC_RLS	99.90	2011
HOG+ CRC_RLS	98.15	480	TT+HOG+ CRC_RLS	99.13	500

3.2 COMPARATIVE STUDY

To validate the importance of obtained results, the following section provides a comparison between the proposed system and some original works in the literatures that are given in Table.4. It can be observed that the proposed framework runs quickly than other methods such as: mean curvature images (MCI), surface type (ST), Gaussian curvature images (GCI) [7] and the local correlation (LC)-based method [8] except with the block-wise features and collaborative representation (CR_L2) [11] method. In the experiment, the costs of the proposed framework require only 0.33 seconds to complete one identification operation taking into account the large data set that comprises 8.000 samples from 400 classes.

Table.4 Comparative of the proposed system with the existing approaches for 3D palmprint

Methods	RR (%)	Runtime for 1 identification (ms)
CR_L2 [11]	99.15	70
LC [8]	91.73	70992.13
ST [7]	98.78	63275.86
MCI [7]	91.88	9403.33
GCI [7]	91.87	9403.33
TT+Gabor+CRC_RLS	100	330

4. CONCLUSION

In this paper, a novel method for 3D palmprint recognition was introduced. A set of preprocessing techniques was applied to a 3D depth image which can effectively and efficiently eliminate the effect of the low-frequency component of the processed image. A dataset of 400 classes was employed. The obtained results clearly demonstrated the ability of the introduced method to outperform other works in the state of the art. It achieved better performance with higher Recognition rate 100% in lowest Runtime. According to the results, it can be concluded that the proposed system is an efficient tool in biometric systems. The main objective of future work is to take advantage of other modalities such as fingerprint and integrating them in order to yield a better performance security system.

REFERENCES

[1] S. Li and A. Jain, "*Encyclopedia of Biometrics*", Springer, 2015.

[2] A. Attia and C. Mourad, "Individual Recognition System using Deep network based on Face Regions", *International Journal of Applied Mathematics, Electronics and Computers*, Vol. 6, No. 3, pp. 27-32, 2018.

[3] N.E. Chalabi, A. Attia and A. Bouziane, "Multimodal Finger Dorsal Knuckle Major and Minor Print Recognition system based on PCANET Deep Learning", *ICTACT Journal on Image and Video Processing*, Vol. 10, No. 3, pp. 2153-2158, 2020.

[4] R. Hammouche, A. Attia and S. Akrouf, "A Novel System based on Phase Congruency and Gabor-Filter Bank for

Finger Knuckle Pattern Authentication", *ICTACT Journal on Image and Video Processing*, Vol. 10, no. 3, pp. 2125-2131, 2020.

[5] A. Attia, M. Chaa, Z. Akhtar and Y. Chahir, "Finger Kunckcle Patterns based Person Recognition via Bank of Multi-Scale Binarized Statistical Texture Features", *Evolving Systems*, Vol. 98, pp. 1-11, 2018.

[6] A. Attia, A. Moussaoui, M. Chaa and Y. Chahir, "Finger-Knuckle-Print Recognition System based on Features Level Fusion of Real and Imaginary Images", *ICTACT Journal on Image and Video Processing*, Vol. 8, No. 4, pp. 1793-1799, 2018.

[7] D. Zhang, G. Lu, W. Li, L. Zhang and N.Luo, "Palmprint Recognition using 3-D Information", *IEEE Transactions on Systems, Man, and Cybernetics, Part C (Applications and Reviews)*, Vol. 39, No. 5, pp. 505-519, 2009.

[8] D. Zhang, V. Kanhangad, N. Luo and A. Kumar, "Robust Palmprint Verification using 2D and 3D Features", *Pattern Recognition*, Vol. 43, No. 1, pp. 358-368, 2010.

[9] J. Cui, "2D and 3D Palmprint Fusion and Recognition using PCA plus TPTSR Method", *Neural Computing and Applications*, Vol. 24, No. 3-4. pp. 497-502, 2014.

[10] A. Meraoumia, S. Chitroub and A. Bouridane, "2D and 3D Palmprint Information, PCA and HMM for an Improved Person Recognition Performance", *Integrated Computer Aided Engineering*, Vol. 20, No. 3, pp. 303-319, 2013.

[11] L. Zhang, Y. Shen, H. Li and J. Lu, "3D Palmprint Identification Using Block-Wise Features and Collaborative Representation", *IEEE Transactions on Pattern Analysis and Machine Intelligence*, Vol. 37, No. 8, pp. 1730-1736, 2104.

[12] M. Chaa, N.E. Boukezzoula and A. Attia, "Score-Level Fusion of Two-Dimensional and Three-Dimensional Palmprint for Personal Recognition Systems", *Journal of Electronic Imaging*, Vol. 26, No. 1, p. 13018-13024, 2017.

[13] W. Li, D. Zhang, G. Lu and N. Luo, "A Novel 3-D Palmprint Acquisition System", *IEEE Transactions on Systems, Man, and Cybernetics Part A: Systems and Humans*, Vol. 42, No. 2, pp. 443-452, 2011.

[14] J.C. Russ and R.P. Woods, "Book Review. The Image Processing Handbook", *Journal of Computer Assisted Tomography*, Vol. 19, No. 6, pp. 979-981, 1995.

[15] X. Tan and W. Triggs, "Enhanced Local Texture Feature Sets for Face Recognition Under Difficult Lighting Conditions", *IEEE Transactions on Image Processing*, Vol. 19, No. 6, pp. 1635-1650, 2010.

[16] T. Zhang, Y.Y. Tang, B. Fang, Z. Shang and X. Liu, "Face Recognition under Varying Illumination using Gradient Faces", *IEEE Transactions on Image Processing*, Vol. 18, No. 11, pp. 2599-2606, 2009.

[17] B. Wang, W. Li, W. Yang and Q. Liao, "Illumination Normalization based on Weber's Law with Application to Face Recognition", *IEEE Signal Processing Letters*, Vol. 18, No. 8, pp. 462-465, 2011.

[18] H. Wang, S.Z. Li, Y. Wang and J. Zhang, "Self Quotient Image for Face Recognition", *Proceedings of International Conference on Image Processing*, pp. 1397-1400, 2004.

[19] L. Shen and L. Bai, "A Review on Gabor Wavelets for Face Recognition", *Pattern Analysis and Applications*, Vol. 9, No. 2-3, pp. 273-292, 2006.

[20] L. Zhang, M. Yang and X. Feng, "Sparse Representation or Collaborative Representation: Which Helps Face Recognition?", *Proceedings of International Conference on Computer Vision*, pp. 471-478, 2011.

[21] N. Dalal and B. Triggs, "Histograms of Oriented Gradients for Human Detection", *Proceedings of International Conference on Computer Vision and Pattern Recognition*, pp. 886-893, 2005.

[22] D. Zhang, W.K. Kong, J. You and M. Wong, "Online Palmprint Identification", *IEEE Transactions on Pattern Analysis and Machine Intelligence*, Vol. 25, No. 9, pp. 1041-1050, 2003.